ACS APPLIED MATERIALS & INTERFACES

Research Article

www.acsami.org

Thermo-Induced Shape-Memory PEG-PCL Copolymer as a Dual-Drug-Eluting Biodegradable Stent

Chien-Shen Yang,[†,#] Hsi-Chin Wu,[‡,#] Jui-Sheng Sun,[§] Hao-Ming Hsiao,[∥] and Tzu-Wei Wang*[,†,⊥]

[†]Department of Materials Science and Engineering, National Tsing Hua University, Hsinchu 30013, Taiwan

[‡]Department of Materials Engineering, Tatung University, Taipei 104, Taiwan

[§]Department of Orthopedic Surgery, National Taiwan University Hospital—Hsinchu Branch, Hsinchu 30013, Taiwan

[∥]Department of Mechanical Engineering, National Taiwan University, Taipei 10617, Taiwan

[⊥]Institute of Biomedical Engineering, National Tsing Hua University, Hsinchu 30013, Taiwan

Supporting Information

ABSTRACT: In this work, a thermo-induced shape-memory drug-eluting stent (SMDES) has been developed by cross-linking PEG-PCL copolymer (cPEG-PCL). The stent is able to perform the shape-memory effect from a temporary linear form to a permanent spiral shape with the transition temperature close to body temperature. The stent incorporates a controlled dual drug-release system for the purpose of preventing in-stent restenosis of the vessel for short- and long-term therapeutic effects. From the results, ^{1}H NMR and GPC indicate that the compositions of PEG-PCL block copolymers are similar to the feed ratios of PEG/ε-CL. A Young's modulus of the cPEG-PCL stent can be achieved that ranges from tens to one hundred megapascals by modulation of the mixing ratio of PEG/PCL. The cPEG-PCL stent is demonstrated to recover to its permanent shape with a high fixing ratio (>99%), recovery ratio (>90%), and recovery time (<10 s). DSC data reveals that the transition temperature is around body temperature (40 °C). Cytotoxicity tests prove that the cPEG-PCL_6040 stent has good biocompatibility. In vitro degradation tests show that the cPEG-PCL_6040 stent undergoes a bulk degradation of 47% after 60 days of incubation under flow conditions. Platelet adhesion and smooth muscle cell proliferation were significantly inhibited by coculture with a mitomycin C/curcumin-eluting stent as a result of the release of curcumin for antiplatelet adhesion during the initial 2 weeks followed by long-term inhibition of smooth muscle cell hyperproliferation for 60 days via mitomycin C. After 60 days of incubation in a bioreactor, the appearance of the stent remains intact and shows no signs of recoiling or collapse.

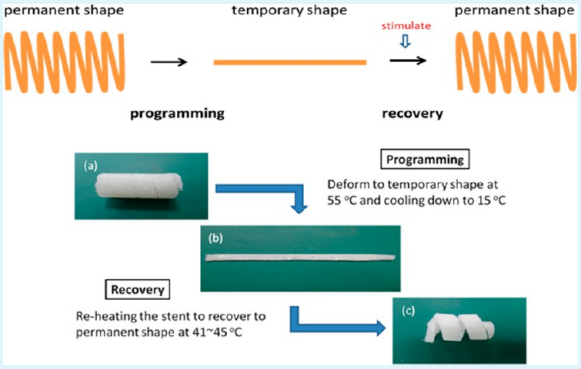

KEYWORDS: *shape-memory effect, biodegradable, drug delivery, polymer, stent*

INTRODUCTION

The treatment of coronary artery disease using vascular stents is one of the most revolutionary medical interventions.[1] Over the past 2 decades, percutaneous transluminal coronary angioplasty (PTCA) with bare-metal-stent placement has been utilized as a minimally invasive treatment for vascular diseases. However, after 6 months, a renarrowing of the treated artery is commonly observed in patients. This renarrowing of the treated artery is due to in-stent restenosis, which is the major drawback of PTCA, occurring in 10−40% of patients.[2] Restenosis following PTCA has been shown to result from three processes, including early elastic recoil, negative vessel remodeling, and neointimal hyperplasia.[3] It is generally believed that in-stent restenosis is mainly caused by neointimal hyperplasia of smooth muscle cells (SMCs).[4] Many approaches have been researched to prevent in-stent restenosis, and drug-eluting stents (DESs) are recent innovations for intravascular treatment.[5,6] A DES is a stent that is coupled with the local delivery of drugs that has demonstrated a tremendous effect on reducing restenosis rates. The clinical importance of drug-eluting stents was demonstrated by their unparallel success in preventing in-stent restenosis after stenting procedures. From the time that they were first used, two generations of DES have been launched.[7,8] Most representative drugs used in DESs are antiproliferative agents such as rapamycin and its derivatives, which have been shown to inhibit SMC proliferation in in vitro experiments and to reduce neointimal formation in injured vessels.[9,10] Incorporation of antiplatelet drugs (antiaggregants) with a DES is another choice for stent pharmacology. Antiplatelet drugs, including aspirin, heparin, and clopidogrel, can decrease platelet aggregation and reduce thrombus formation.[11]

Received: August 5, 2013
Accepted: October 10, 2013
Published: October 10, 2013

Considering the short-term need as well as the potential for long-term complications with metallic stents, stents made of biodegradable polymeric materials may be an ideal alternative choice. Shape-memory polymers (SMPs) have gained increasing attention over the last several years for use as a proposed biomaterial for minimally invasive surgical devices. SMPs are stimulus-responsive materials that have the ability to change their shape upon application of an external stimulus. They are able to be fixed in a temporary shape and to recover their permanent shape when triggered by an external stimulus. Heat-induced shape-memory polymers have drawn the most attention because they can change shape by changing the temperature.[12] They can recover to their permanent shape upon heat activation above their transition temperature. If the transition temperature is around body temperature, then it has promising potential for use in biomedical applications.

Shape-memory polymers can be used in biomedical applications such as cardiovascular stents, sutures,[13] clot cleaners,[14] and drug-delivery systems,[15] depending on it shape-memory functionality. Yakacki and his co-workers developed shape-memory polymer stents from *tert*-butyl acrylate (tBA) and poly(ethylene glycol) dimethacrylate (PEGDMA).[16] The stent can be programmed to be activated at body temperature, resulting in a natural deployment without the need for auxiliary devices. The limitation was its nonbiodegradability. There are also some research works in the investigation of biodegradable polymer-based stents. However, most biodegradable polymer-based stents result in some problems during their degradation. For example, degradation of acid−base polymers such as PLGA results in a significant pH change because of the release of acid that leads to the necrosis of surrounding cells.[17] Moreover, some biodegradable polymers are not equipped with enough mechanical strength to afford long-term erosion by the bloodstream and the pressure applied by vessel wall.[18] The stent may collapse into small pieces before complete degradation because of insufficient mechanical strength. The small pieces will block the vessel, causing severe complications such as stroke.

The objective of this study is to develop a thermo-induced, biodegradable shape-memory drug-eluting stent (SMDES) with dual drug-release profiles that can sustainably release mitomycin C (antiproliferative drug) and curcumin (anticoagulant drug) after shape-memory performance. Thus far, although some research studies have incorporated the shape-memory effect with a vascular stent, the transition temperature is still high, and the stent is mostly nonbiodegradable. For this reason, we prepared a cross-linked PEG-PCL shape-memory stent with a transition temperature around body temperature. In addition, different drug-carriage systems were created to prevent the temporal sequence of thrombosis formation and SMC hyperproliferation. The in vitro characteristics of the shape-memory functionality of SMDES were evaluated, including biocompatibility, drug-release profiles, and antirestenotic effects. A biomimetic bioreactor was prepared to mimic the in vivo vascular flow conditions to monitor the degradation and integrity of SMDES after long-term pulsatile flushing. Incorporation of the shape-memory effect with polymer stents can prevent early elastic recoil and negative vessel remodeling after stent implantation. Furthermore, a linear temporary shape can be delivered to a constricted vessel and can recover to its spiral permanent shape after being activated above body temperature without the need for auxiliary devices. With different mechanisms of vessel dilation, shape-memory stents can resist the radial force applied by the vessel wall more than stents implanted by PTCA.

EXPERIMENTAL SECTION

PEG (M_w = 6 kDa), ε-caprolactone (ε-CL, 99%), and stannous octoate were purchased from Sigma-Aldrich. Benzoyl peroxide (BPO), succinic anhydride (SA, 99%), and 4-(dimethylamino)pyridine (DMAP) were ordered from Alfa Aesar. 1-Ethyl-3-(3-dimethylaminopropyl) carbodiimide hydrochloride (EDC) and *N*-hydroxysuccinimide (NHS) were obtained from Fluka and Sigma-Aldrich, respectively. Curcumin (98%) and mitomycin C (from *Streptomyces casepitosus*) were supplied by Sigma-Aldrich. All reagents were used as received without any further purification. All other reagents used in this study were analytical grade.

Synthesis of PEG-PCL Block Copolymers and Modification of the Carboxylic Acid Group on PCL. PEG-PCL block copolymers were produced with ε-CL monomer and PEG (M_n = 6000) via polycondensation using stannous octoate as the catalyst.[19] ε-CL monomer was dried in a three-necked flask under vacuum at room temperature for 2 h before polymerization. Different weight ratios of PEG/ε-CL were prepared and reacted with 0.1 wt % stannous octoate under vacuum with mechanical stirring at 160 °C for 4 h. After cooling to room temperature, the resulting copolymers were dissolved in dichloromethane and precipitated in an excess of cold ether. The precipitated PEG-PCL copolymer was then dried at room temperature under vacuum for further use.

Modification of the carboxylic acid group on PCL was carried out in the presence of succinic anhydride (SA) and 4-dimethylaminopyridine (DMAP).[20] PEG-PCL block copolymers were dissolved in dimethylformamide (DMF) followed by the addition of SA and DMAP. The mixture was stirred overnight under a nitrogen atmosphere at room temperature. After completion of the reaction, the resulting PEG-PCL copolymer was precipitated and again dried at room temperature under vacuum for use in experiments.

Cross-Linking of PEG-PCL Copolymers and Stent Fabrication. PEG-PCL copolymers were cross-linked through free-radical polymerization by benzoyl peroxide (BPO).[21] PEG-PCL copolymer and 15 wt % of the cross-linking agent BPO were dissolved in dichloromethane and dried under vacuum overnight. Different amounts of the mixture were added into a preformed stainless mold for the cross-linking process. The stainless mold containing the mixture was placed into an oven, and the temperature was increased to 140 °C for 10 min to activate the cross-linking reaction. After cooling to room temperature, the cross-linked PEG-PCL (cPEG-PCL) stent was obtained. The final stent is shown in Figure 1a and has an inner diameter of 5 mm and an outer diameter of 9 mm.

Physiochemical Property Analysis by ^{1}H NMR, Differential Scanning Calorimetry (DSC), Gel-Permeation Chromatography (GPC), and Universal Mechanical Tester. ^{1}H NMR spectra were used to determine the compositions and molecular weights of PEG-PCL and the modified PEG-PCL copolymers. $CDCl_3$ was used as the solvent, and TMS was used as the internal standard for the measurement using a Varian Unityinova 500NMR at 25 °C. The actual PEG/PCL ratio of PEG-PCL copolymer and the modification efficiency were calculated from the integral height of specific representative hydrogen peaks shown in the ^{1}H NMR spectra.

Thermal behavior, such as the melting temperature of PEG-PCL and cross-linked PEG-PCL copolymers, was investigated precisely with a PerkinElmer differential scanning calorimeter (DSC220C, PerkinElmer) using polymer that was encapsulated in aluminum pans. The operation was carried out at a heating rate of 10 °C/min under a nitrogen atmosphere from 25 to 100 °C using 5 mg of each sample. Nitrogen was used as the purge gas with a flow rate of 40 mL/min.

The molecular weight, M_n, and polydispersity index, PDI, of PEG-PCL copolymers were analyzed by gel-permeation chromatography (GPC) consisting of a high-performance liquid chromatography (HPLC) pump (PU-2080, Jasco) with a refractive-index detector (RI-2031, Jasco) and an injection valve (7725i, Rheodyne) with a 20

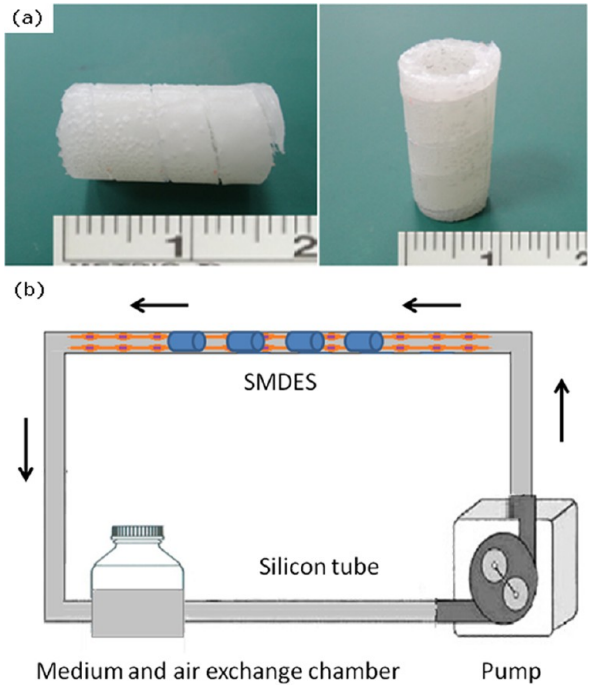

Figure 1. (a) Photos of the cross-linked PEG-PCL_6040 shape-memory stent. (b) Schematic illustration showing the bioreactor for mimicking in vivo vessel conditions under pulsatile flow. The bioreactor consists of three parts: a peristaltic pump, silicon tubes, and an air-exchange chamber. Using a peristaltic pump, the stent was subjected to a continuous flow (500 mL/min) of hSMC culture medium at 37 °C.

μL sample loop. THF was used as the solvent at a flow rate of 1.0 mL/min. The molecular weight and PDI were determined relative to polystyrene standards.

For measurements of tensile properties, an Instron tensile tester (8848 series, with extensometer) was employed. The standard dumbbell-shaped specimens by the regulation of ASTM-D638 were strained under wet conditions at a constant rate of 10 mm/min until failure. The reported values of tensile modulus and strength are based on initial dimensions. All experiments were conducted in at least triplicate and were reproducible.

Characterization of the Shape-Memory Behaviors of Cross-Linked PEG-PCL Stents. Shape-memory experiments of cross-linked PEG-PCL stents were performed by a thermal chamber with a camera. All experiments were conducted in at least triplicate and were reproducible. The experiments consisted of heating the permanent spiral shape above the transition temperature, deforming to the temporary linear shape, cooling to the storage temperature (15 °C), and reheating the temporary linear shape to recover the permanent spiral shape. Critical parameters of shape-memory behaviors, including the fixing ratio (R_f), recovery ratio (R_r), and recovery time (R_t), were demonstrated by calculation and video recording. The fixing ratio and recovery ratio were obtained by calculation of the projection length before and after programming and recovery, respectively.

$R_f = L_f/L_0$ and $R_r = L_r/L_0$, where L_0 is the original projection length, L_f is the projection length after programming, and L_r is the projection length after recovery.

Degradation of Cross-Linked PEG-PCL Stents in Vitro. Degradation experiments were carried out under flow and static conditions, respectively. The starting mass of the samples was 0.5 g. The dimensions of the sample films were 10 × 40 × 2 mm^3. The degradation rates were estimated from the weight loss of the specimens. Stents were immersed in a 0.1 M phosphate buffer solution (PBS, pH 7.4) at 37 °C. After predetermined time intervals, the stents were taken out, washed with distilled water, and dried under vacuum. Weight loss was calculated with the following equation: weight loss (%) = $100 \times [1 - (W_t/W_0)]$, where W_0 and W_t are the dry stent weight before and after degradation, respectively.

Cytotoxicity Test by LDH Assay. A LDH assay was used to test the cytotoxicity of the cPEG-PCL stents. The size of the sample films was 5 × 5 mm^2. Mouse 3T3 fibroblasts were cultured in DMEM high-glucose medium containing 1% PSA and 10% FBS. The cell seeding density was 5×10^4 cells/cm^2. LDH activity was measured in the culture medium by an enzymatic method at 490 nm using a multifunction spectrophotometer. LDH assessments were implemented according to LDH handbooks provided by G-Biosciences and were performed on day 2.

Preparation of the Mitomycin C/Curcumin-Eluting Stent and Measurement of the in Vitro Drug-Release Profile. The mitomycin C/curcumin-eluting stent was prepared first by conjugation of mitomycin C followed by coating of curcumin to the stent. Mitomycin C was chemically cross-linked by EDC/NHS, whereas curcumin was then coated on cPEG-PCL stents with the use of agarose gel. In brief, mitomycin C, EDC, and NHS were dissolved in DI water (EDC/NHS, 5:2 molar ratio), and the cPEG-PCL stents were immersed into solution for 4 h at pH 5.5. After conjugation, cPEG-PCL stents were washed with DI water to remove the unreacted EDC, NHS, and mitomycin C. Agarose was dissolved in DI water and heated to 100 °C. After cooling to 50 °C, it was mixed with curcumin. Meanwhile, the cPEG-PCL stent was immersed into the solution for 20 s and held there until gelation layer formation.

All stents (1.5 cm in length × 1 cm in width) were incubated in 15 mL of a 0.1 M phosphate buffer solution (PBS, pH 7.4) at 37 °C. After predetermined time intervals, the incubation medium was completely removed for analysis and replaced with the fresh PBS. Detection and quantitative analysis of drug release were performed using a multifunction spectrophotometer at 535 nm for curcumin and 595 nm for mitomycin C, respectively.

Antiplatelet Adhesion Examination and Inhibition of hSMCs Proliferation. cPEG-PCL films were cut into 8 mm discs by biopsy punch and sterilized by immersion in 75% ethanol. To inhibit platelet adhesion, a therapeutic concentration of curcumin was coated on to cPEG-PCL discs to achieve an effective dose of 10 μM/day. Curcumin-coated discs were placed into a 48-well culture plate with 300 μL of fresh platelet-rich plasma (PRP) and cultivated at 37 °C. PRP was renewed on days 5 and 10. cPEG-PCL discs with a pure agarose coating were chosen as the control. At predetermined time intervals (days 1, 3, 7, and 14), the samples were washed with PBS to remove the nonadherent platelets. The discs were then soaked in 2% glutaraldehyde for 30 min followed by 5% glutaraldehyde for 120 min to fix the adhered platelets. After washing with PBS, the discs were dehydrated in a series of ethanol–water solutions (50, 50, 75, 90, and 100%) and allowed to dry in a vacuum oven. The platelet-attached surfaces were gold-deposited and examined by scanning electron microscopy (SEM).

For the proliferation test of hSMCs and hUVECs, curcumin and mitomycin C with different concentrations were applied to cPEG-PCL discs to determine the optimal effective dose for future applications. cPEG-PCL discs without drugs were chosen as the control group. Sample and control discs were placed in 48-well culture plates. hSMCs (ATCC, no. CRL-1999) and hUVECs (BCRC, no. H-UV001) were seeded at a density of 10^4 cells/cm^2 and cultured with modified Ham's F-12K medium and Medium 500 with modifications, respectively. At predetermined time intervals, cell number determinations were performed by cell proliferation MTS assay. The absorbance of formazan, measured at 490 nm is directly proportional to the number of living cells in culture.

Bioreactor System Configuration. To mimic in vivo vessel conditions, a peristaltic bioreactor system was prepared as shown in Figure 1b. Silicon tubes were coated with laminin and then seeded with hSMCs. Mitomycin C/curcumin-eluting stents were implanted into the tube connected to the peristaltic pump, and the entire system was primed with SMC culture medium and placed in an incubator. A flow rate of 500 mL/min was obtained, which was chosenon the basis of comparable equivalent rates in an artery.[22] The degradation degree and morphology of the stent after flushing for 60 days were estimated

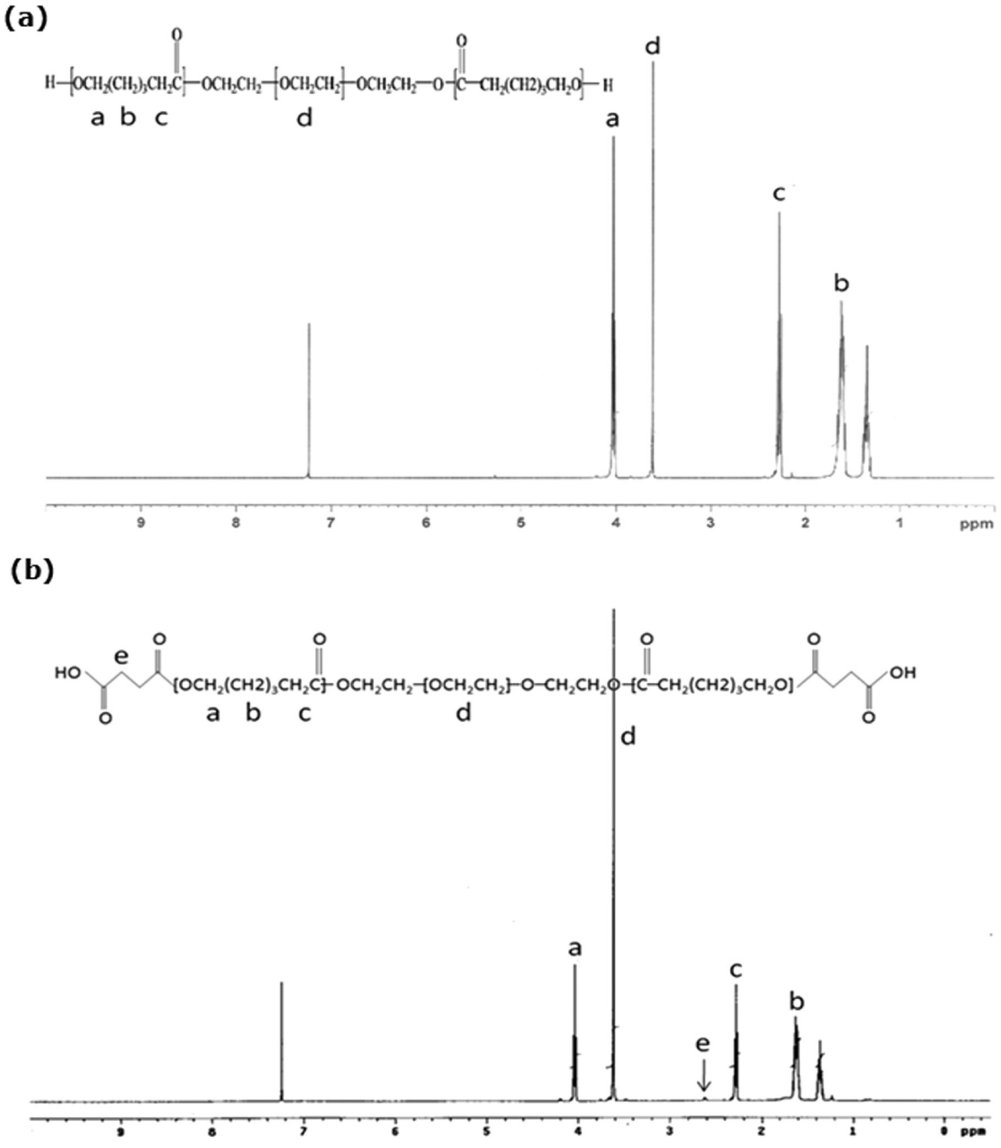

Figure 2. ^{1}H NMR spectrum of (a) PEG-PCL_6040 block copolymers and (b) carboxylic acid group-modified PEG-PCL_6040 copolymers.

from the weight loss and histology analysis. The stent integrity was also photographed for comparison.

RESULTS

Characteristics of PEG-PCL Copolymer and Cross-Linked PEG-PCL Stent. PEG-PCL copolymers were prepared with different ε-CL/PEG weight ratios (PEG-PCL_2080, PEG-PCL_4060, PEG-PCL_6040, and PEG-PCL_8020) to control the degradation rate and to optimize the shape-memory functionality. The ^{1}H NMR spectra of a typical PEG-PCL_6040 block copolymer is shown in Figure 2a. For PCL units, peaks at 1.62, 2.34, and 4.09 ppm were attributed to $-(CH_2)_3-$, $-CH_2CO-$, and $-OCH_2-$, respectively. The peak at 3.66 ppm was attributed to the methylene protons of homosequences of the PEG oxyethylene units ($-OCH_2CH_2-$). The M_w of the PEG-PCL copolymers and the weight ratios of PEG/PCL in the copolymers were calculated by comparing integrations of PCL methylene at 4.09 ppm and PEG methylene at 3.66 ppm. The constituted weight ratio of these copolymers was similar to the feed ratio of the individual monomer, as shown in Table 1. The M_w of the PEG-PCL copolymers was also determined by GPC for comparison with the result obtained by ^{1}H NMR.

The ^{1}H NMR spectra of PEG-PCL copolymers with the carboxylic acid group modified is shown in Figure 2b. It confirmed succinoylated PEG-PCL characteristic peaks through the aliphatic protons of succinoyl moiety at 2.5−2.7 ppm. The modification efficiency of the PEG-PCL copolymers was 72%,

Table 1. Compositions and Molecular Weights of PEG-PCL Block Copolymers

	weight ratio (PEG/PCL)		molecular weight		
	feed	actual[a]	M_n[a]	M_n[b]	PDI[c]
PEG-PCL_2080	20:80	17:83	38 000	39 323	1.35
PEG-PCL_4060	40:60	36:64	22 000	21 346	1.37
PEG-PCL_6040	60:40	63:37	11 000	10 132	1 32
PEG-PCL_8020	80:20	79:21	8000	8201	1.33

[a]Determined by ^{1}H NMR measurement in $CDCl_3$. [b]Determined by GPC measurement in THF. [c]PDI is the polydispersity index, which is equal to M_w/M_n.

which was calculated by comparing integrations of aliphatic protons of the succinoyl moiety at 2.5−2.7 ppm and PEG methylene at 3.66 ppm.

The DSC curve of PEG-PCL_6040 copolymers before and after cross-linking are shown in the Supporting Information, Figure 1. The thermal property data are summarized in Table 2.

Table 2. Thermal Properties of PEG-PCL and Cross-Linked PEG-PCL Copolymers[a]

	T_m (°C)	crystallinity (%)	T_{onset} (°C)
PEG-PCL_2080	60.33	56.7	51.56
PEG-PCL_4060	60.13	50.8	52.33
PEG-PCL_6040	57.48	52	51.58
cPEG-PCL_2080	52.31	33.2	41.95
cPEG-PCL_4060	51.65	29.8	40.67
cPEG-PCL_6040	51.97	30.1	40.98

[a]cPEG-PCL, cross-linked PEG-PCL copolymer.

PEG-PCL copolymers exhibit a T_m around 60 °C for the three mixing ratio groups. After cross-linking, a drop in the T_m from 60 to 50 °C for the cPEG-PCL copolymers was observed. This can be attributed to the decreased crystallinity, which was calculated using the heat of fusion of 100% crystalline PCL and PEG. Of note is that for all cross-linked PEG-PCL stents the onset temperature (T_{onset}) of the melting transition was 11 °C lower than the T_m. The T_{onset} of cPEG-PCL_6040 was about 41 °C, suggesting that the cPEG-PCL_6040 stent possessed the capability of performing its shape-memory effect at a temperature close to body temperature.

Mechanical Properties and Shape-Memory Behaviors of Cross-Linked PEG-PCL Stents. The results of tensile tests under wet conditions at 37 °C are shown in Table 3. The Young's modulus and ultimate tensile strength of cPEG-PCL stents decreased with the increase of the PEG content. The Young's modulus of cPEG-PCL_2080, cPEG-PCL_4060, and cPEG-PCL_6040 are 97.2, 49.4, and 28.2 MPa, respectively. This range of mechanical strength is comparable to previous research and may be strong enough to resist the recoiling and collapse of the expanded stent after implantation.[28]

The shape-memory process of the cPEG-PCL stent is demonstrated in Figure 3. The experimental process consisted of heating the stent at 55 °C, deforming it to the temporary linear shape, cooling to 15 °C for 15 min, and then reheating the temporary linear shape to 41−45 °C to recover the permanent spiral shape. Shape-memory behaviors, including the fixing ratio (R_f), recovery ratio (R_r), and recovery time (R_t), of the cPEG-PCL stents are outlined in Table 3. The results showed that R_f was near 100% for all weight ratios. R_r was 99.5% for PEG-PCL_2080, 96.25% for PEG-PCL_4060, and 87.5% for PEG-PCL_6040. For R_t, all of the stents could recover to the permanent shape within 10 s, suggesting a good shape-memory functionality of the fabricated cPEG-PCL stents.

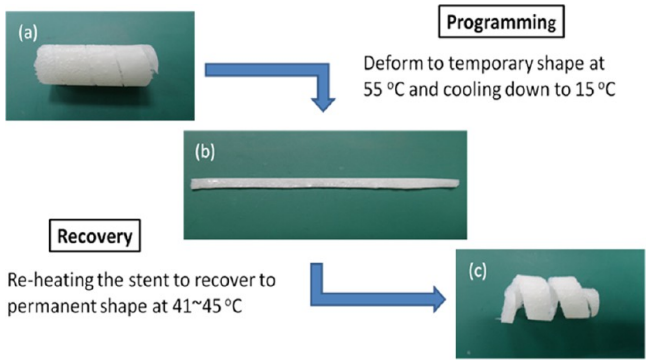

Figure 3. Photographs demonstrating the shape-memory effect of a cross-linked PEG-PCL_6040 stent. (a) Permanent shape of the stent, (b) temporary shape of the stent, (c) recovery to the permanent shape of the stent after thermal stimulation.

Degradation and Biocompatibility of Cross-Linked PEG-PCL Stent in Vitro. Figure 4a illustrates the weight loss of cross-linked PEG-PCL stents with incubation time under either static or flow conditions. Under static conditions, an initial weight loss resulting from the hydrolysis of PEG was observed, especially for cPEG-PCL_6040, at an early incubation time within 2 weeks followed by the slow degradation of PCL during the latter period of time for a total of 120 days. A 40% weight loss for cPEG-PCL_6040 was noticed after 120 days of culture under static conditions. When comparing the weight loss of cPEG-PCL_6040 under static and flow conditions, the degradation rate under flow conditions was significantly faster than that of static conditions after 30 days. The degradation of cPEG-PCL_6040 under flow conditions was nearly 50% after 120 days.

The cytotoxicity result, in terms of the LDH assay, of the cPEG-PCL_6040 stent is shown in Figure 4b. Not much difference can be seen between the experimental (cPEG-PCL_6040 stent) and negative control groups. This result indicated that the cPEG-PCL stent has low cytotoxicity.

In Vitro Release of Mitomycin C/Curcumin-Eluting Stents. The in vitro release profiles of mitomycin C and curcumin are plotted in Figure 4c. The stents sustainably released mitomycin C for more than 60 days because of the chemical cross-linking conjugation process, whereas curcumin was eluted more quickly within the initial 14 days because of the physical absorption by the gel-coating process. In the curcumin release profile, the cumulative percentage was approximately 90% after 14 days incubation. The early release of curcumin can prevent initial platelet adhesion and further reduce thrombosis formation. For the cumulative percentage of mitomycin C release, the collected value was approximately 90% after 70 days. This long-term release of mitomycin is able to inhibit smooth muscle cell hyperproliferation, reducing the possibility of in-stent restenosis. The effect of antiplatelets

Table 3. Mechanical Properties and Shape-Memory Behaviors of Cross-Linked PEG-PCL Stents

	ultimate tensile strength (MPa)	Young's modulus (MPa)	R_f (%)[a]	R_r (%)[b]	R_t (sec)[c]
cPEG-PCL_2080	6.4 ± 0.53	97.2 ± 5.21	~100	99.5 ± 1.0	9 ± 0.5
cPEG-PCL_4060	2.9 ± 0.77	49.4 ± 4.49	~100	96.25 ± 1.5	10 ± 0.3
cPEG-PCL_6040	1.1 ± 0.35	28.2 ± 2.31	~100	87.5 ± 2.3	10 ± 0.5

[a]R_f, fixing ratio. [b]R_r, recovery ratio. R_f and R_r values were determined by a thermomechanical tensile test by heating at 55 °C, cooling to 15 °C, and heating again at 41−45 °C. [c]R_t, recovery time

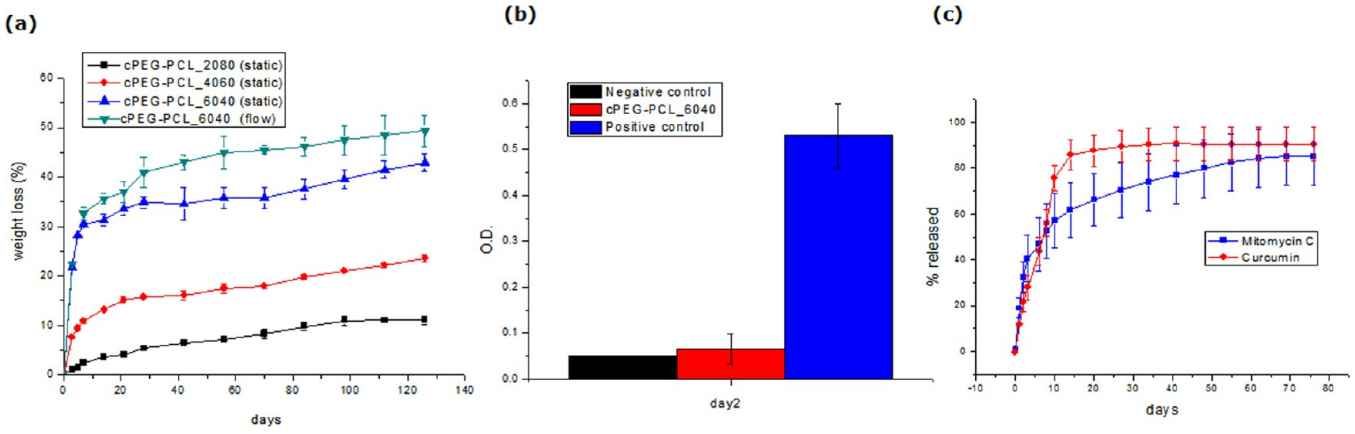

Figure 4. (a) Degradation of cross-linked PEG-PCL stents under static and flow conditions. (b) Biocompatibility of the cross-linked PEG-PCL_6040 stent. The positive control shows the total lysis of all cells, and the negative control shows the spontaneous release of LDH by 3T3 cells in the absence of the cPEG-PCL_6040 stent. (c) Cumulative release profile of the mitomycin C/curcumin-eluting stents. (n = 4).

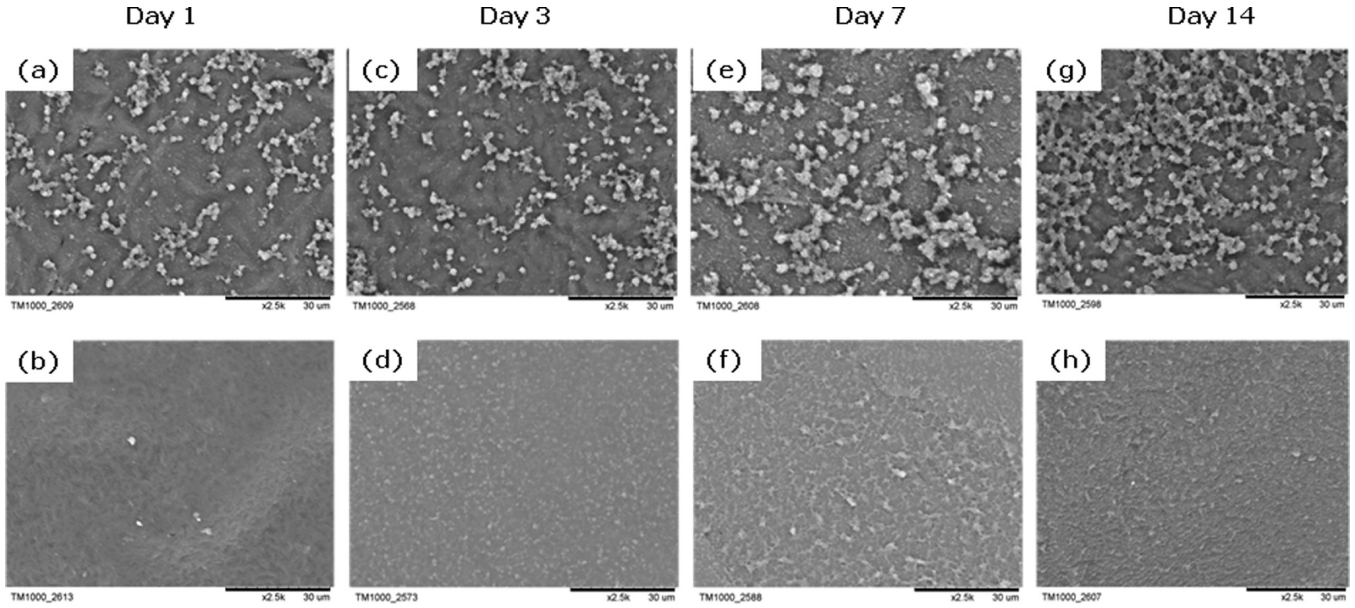

Figure 5. SEM images of the antiplatelet adhesion effect at different time points. (a, c, e, g) cPEG-PCL_6040 stent without drugs and (b, d, f, h) cPEG-PCL_6040 stent with mitomycin C/curcumin.

adhesion and antiproliferation of smooth muscle cells were revealed in the following experiments.

Anticoagulant and Antiproliferation Effect of Shape-Memory Dual-Drug-Eluting Stents. A platelet adhesion experiment was used to evaluate the in vitro anticoagulation effect of mitomycin C/curcumin-eluting stents. In the case of the control cPEG-PCL stent without drugs incorporation, platelet aggregation was clearly observed on the surface of the film by SEM images (Figure 5). For the curcumin-coated cPEG-PCL group, the number of adhered platelets significantly decreased, and the antiplatelet adhesion effect was sustained for at least 14 days.

The behavior of hSMCs and hUVECs cocultured with mitomycin C/curcumin-eluting stents were studied by a cell-proliferation MTS assay for 28 days (Figure 6). Inhibition of SMCs proliferation is a critical factor in preventing neointima formation and thus in-stent restenosis. However, simultaneous inhibition of endothelial cell growth is regarded as detrimental because retarded endothelialization increases the chance for stent thrombosis. Therefore, we attempted to identify an optimal concentration of the drugs that would significantly inhibit hyperproliferation of SMCs but not influence the survival of ECs. For the tested concentrations of curcumin and mitomycin C, the groups of 10 μM/200 nm and 5 μM/100 nm (curcumin/mitomycin C, respectively) significantly suppressed hSMCs proliferation up to 67%, whereas the groups of 2.5 μM/50 nm and 1 μM/20 nm were not able to efficiently inhibit the growth of hSMCs. Also, the treatment with mitomycin C/curcumin-eluting stents at a dosage of 10 μM/200 nm resulted in extensive inhibition of hUVECs viability. However, this did not happen in the group with 5 μM/100 nm; therefore, this concentration should be chosen for future in vivo study. This concentration was also suggested to achieve a therapeutic level for application in restenosis prevention. This finding has important implications for developing drug-eluting stents because a minor responsiveness of endothelial cells to the antiproliferative effect of mitomycin C/curcumin-eluting stents is desirable and appreciated when designing a drug-eluting stent.

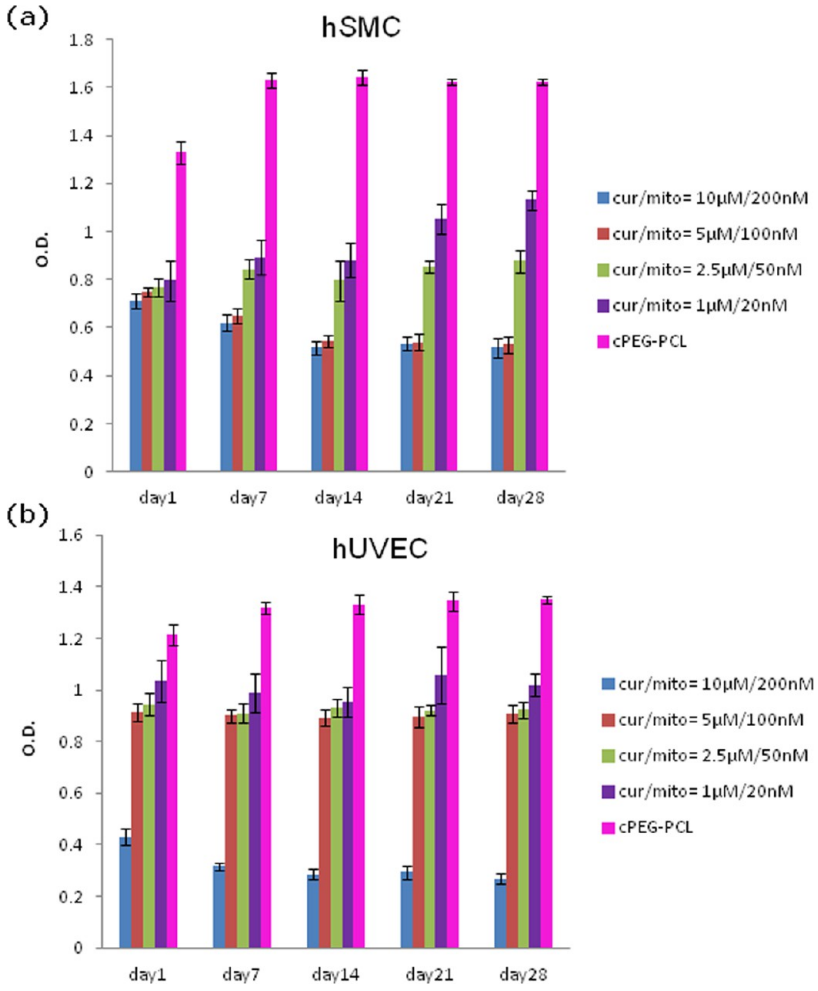

Figure 6. Antiproliferation effect of mitomycin C/curcumin-eluting cPEG-PCL_6040 stent for (a) hSMC and (b) hUVEC. (n = 4).

Biomimic Bioreactor System. Stent integrity under flow conditions in a bioreactor with flushing for 1 or 2 months is presented in Figure 7b,c. As can be seen, the overall morphology was well preserved without significant collapse or damage as compared with the original stent (Figure 7a). From the histology observed in the H/E stain, a porous structure was clearly observed in the inner area of the cPEG-PCL_6040 stent, and this phenomenon was more apparent after 2 months of flushing incubation in a pulsatile bioreactor. By analyzing the result, we propose that bulk degradation instead of surface degradation of the stent occurred, which was very useful and important because if surface corrosion dominated in the degradation process, then the possibility of thrombosis and even severe stroke may exist unexpectedly for the long-term clinical use. From Figures 7d and 7e, it was shown that the cPEG-PCL_6040 stent maintained most of its integrity during degradation. We may modulate the PEG/PCL mixing ratio and cross-linking degree to prolong the degradation rate as necessary.

DISCUSSION

Characteristics of the PEG-PCL Copolymers and Cross-Linked PEG-PCL Shape-Memory Stent. The permanent presence of a stent may lead to complications such as exaggerated inflammatory responses and neointimal hyperplasia at the stent site.[29] Therefore, stents with a biocompatible and biodegradable polymer coating or biodegradable polymer-based stents are preferred and desired to prevent these unfavorable effects.[27] As is known, PCL has a degradation time of more than 2 years without the aid of enzymes.[30] The incorporation of PEG into PCL network can accelerate the degradation rate of PCL and increase the biocompatibility of the copolymer.[31] PEG can spontaneously decompose from large molecules into small molecules under physiological conditions by hydrolysis. The decomposition of PEG turns the cross-linked PEG-PCL copolymers into small molecules and further increases the degradation rate of PCL (Figure 4). Different weight ratios of PEG and PCL in the copolymer may contribute to different degradation rates. The controllable degradation rate is useful for various biomedical applications.

Thermal properties are crucial parameters to create a heat-induced shape-memory stent. In general, a shape-memory effect can be activated above the transition temperature. Here, the melting temperatures (T_m) were the transition temperatures summarized in Table 2, which showed that the melting temperatures decreased from 60 to 50 °C after cross-linking in three PEG/PCL mixing groups because of the decrease of crystallinity. We further found that the shape-memory effect can be triggered at a lower temperature, called the onset temperature (T_{onset}), which was the temperature that the molecular chain started to melt. Once this happened, the polymer became flexible, and the shape-memory effect was activated. From Table 2, it can be seen that the onset temperatures were around 40 °C, which are very close to body

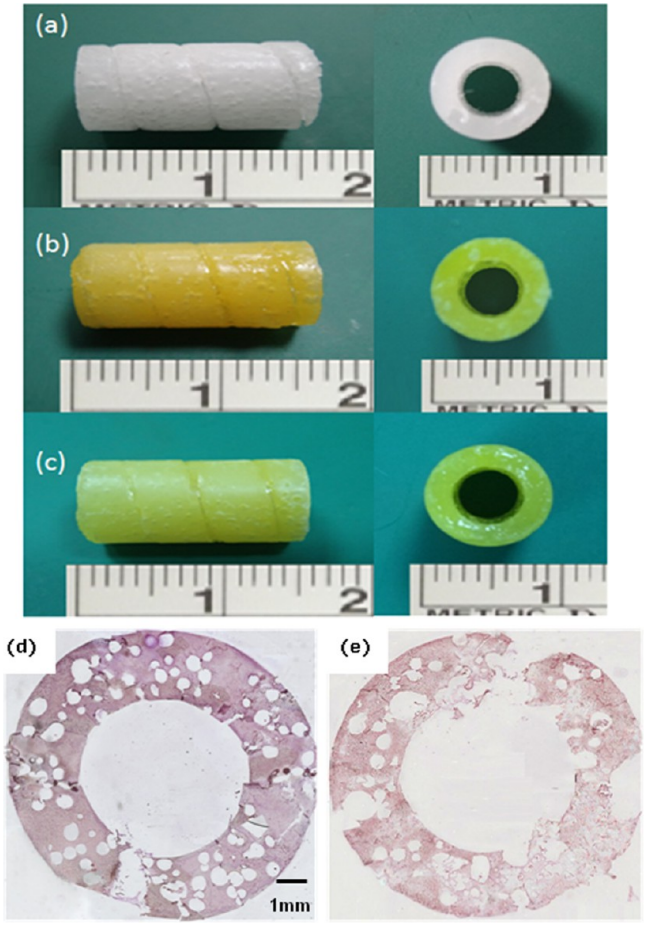

Figure 7. Appearance of the side view and cross-section area after 1 or 2 months of incubation for the cPEG-PCL_6040 shape-memory dual-drug-eluting stent. (a) Original cPEG-PCL_6040 stent and cPEG-PCL_6040 stents after (b) 1 or (c) 2 months of flushing. Histological cross sections of the cEPG-PCL_6040 stent after (d) 1 or (e) 2 months of flushing.

temperature. This indicated that the shape-memory effect can be activated after implanting the polymer into a human body without much concern for cell necrosis caused by the heat-treatment modality.

Until now, there has been no definitive answer for the appropriate mechanical properties and recovery time that a shape-memory stent must have for application in cardiovascular vessels. Compared with previous research studies,[23,24,25] our fabricated cPEG-PCL stent was equipped with comparable mechanical strength. With sufficient mechanical properties, cPEG-PCL stents are able to hold the vascular structure and maintain the lumen area. For a shape-memory material, shape-memory ability is the most critical property. From Table 3, it can be seen that the fabricated cPEG-PCL stent possessed very satisfactory shape-memory behaviors ($R_f \sim 100\%$, $R_r > 90\%$, and $R_t \leq 10$ s). With increasing PCL content, the recovery ratio (R_r) was higher and the recovery rime (R_t) was faster. Different compositions of PEG/PCL (cPEG-PCL_2080, cPEG-PCL_4060, cPEG-PCL_6040, and cPEG-PCL_8020) have been investigated; however, cPEG-PCL_8020 dissolved immediately after immersing in water. Therefore, the remaining groups were used for further studies.

Generally, shape-memory polymers consist of two segments, a switching segment tha provides material flexibility and a hard segment for memorizing the permanent shape. For the cross-linked PEG-PCL shape-memory polymer, the PCL segments cross-linked by BPO are so-called hard segments, and the remaining free chains are switching segments. Cross-linked PEG-PCL shape-memory polymers can recover better and faster to their permanent shape with more hard segments in the polymer network. The R_t value of a shape-memory material is another critical property because a poor recovery rate will lead to difficulty for surgical manipulation of the material in the clinic. From our data, the cross-linked PEG-PCL stent demonstrated a satisfactory shape-memory effect, and the shape-memory property was closely dependent on its composition.

Shape-Memory Dual-Drug-Eluting Stent (SMDES). Restenosis is the renarrowing of a blood vessel causing a reduction of the lumen area and further restricting blood flow after an intervention procedure. It is a combined result of a biological response and a mechanical reaction to percutaneous coronary intervention.[26] The biological responses include platelet adhesion/aggregation, inflammation, thrombosis formation, vascular smooth muscle cells hyperplasia, and late remodeling.[31,32] Curcumin, a major chemical component of turmeric, has proved to be an antiproliferative and anticoagulant drug.[33] Previous research suggests that curcumin can inhibit platelet adhesion and aggregation induced by ADP, epinephrine, and collagen.[34,35] Mitomycin C is a potent inhibitor of vascular SMCs proliferation and neointima formation. Inhibitory abilities of mitomycin C are attributed to the induction of cyclin-dependent kinase inhibitor, p21, and the arrest of vascular SMCs in the G2−M phase of the cell cycle.[36]

In this study, different drug-release profiles were created to try to match the temporal sequences of thrombosis formation and proliferation. A 14 day release profile of curcumin was prepared by gel coating, whereas a 60 day release profile of mitomycin C was obtained by EDC/NHS cross-linking (Figure 4). This combination of release profiles can simultaneously inhibit early thrombotic formation and long-term vascular SMCs overexpression, thus preventing restenosis. In the platelets adhesion experiment, PRP was replaced on days 5 and 10, and the inhibitory effect was sustained for 14 days (Figure 5). For hSMCs proliferation, culture medium was renewed every 3 days, and the proliferation of SMCs was suppressed for at least 28 days (Figure 6). These results indicate that therapeutic doses of curcumin and mitomycin C were released from the stent and may result in the prevention of restenosis.

Heat-induced SMDES can be programmed via thermal activation and can recover to its permanent shape upon heat activation above the transition temperature (Figure 3). Constricted vessels could be dilated during the shape-memory process. In this current study, the developed SMDES is advantageous and very beneficial when implanted by a catheter in a blood vessel and recovered to its permanent stent shape using a temperature close to body temperature as the trigger agent. Even more, balloon-expansion procedures could be added to provide the stent with sufficient mechanical properties and a precise shape if needed. After complete recovery, the recovered stent may serve as a scaffold and further prevent restenosis by releasing drugs. To the best of our knowledge, although some research studies have incorporated a shape-memory effect with a vascular stent, the transition temperature was too high and the stent was not biodegradable.[37] In our

work, a mitomycin C/curcumin-eluting stent was able to recover from a linear temporary shape to a spiral permanent shape at 41−45 °C with excellent shape-memory properties. This dilation process differs from previous research and has clinical-application potential. The spiral shape might also provide better resistance against the radial force applied by the vessel wall compared to a tubular shape because the expansionary force (F_x) of a tubular shape is exactly antiparallel to the constrictive force (F_{-x}) of the vessel wall.[38] With stronger resistance to the radial force of the vessel wall, SMDES can avoid early elastic recoil and negative vessel remodeling, further reducing the possibility of restenosis.

Biomimic Bioreactor System. To mimic in vivo arterial blood-flow conditions, a SMDES was implanted into a self-designed bioreactor with the flow rate of 500 mL/min, which was equivalent to that of arterial blood flow.[39] We found that degradation under biomimicking flow conditions was faster than that under static conditions (Figure 4). Degradation of cPEG-PCL stents under pulsatile flow conditions was attributed to both chemical and enzymatic hydrolysis, and the results were in agreement with previous study.[40] One concern with biodegradable stents is that during the degradation a reduction in the mechanical strength may occur. The implanted stent tends to eventually fail to support the blood vessel wall with the risk of stent recoil or collapse and therefore thrombus formation.[41] From our results after 60 days of incubation in a bioreactor, the appearance of the cPEG-PCL drug-eluting stent remained intact and showed no signs of corrosion or collapse even with 47% weight loss (Figure 7). The histological finding also showed that the cPEG-PCL stent was in bulk degradation under biomimicking physiological conditions and would be capable of sustaining the dilated vessel against restenosis for a prolonged period of time in future in vivo applications.

CONCLUSIONS

In this study, we have successfully synthesized PEG-PCL copolymers with different weight ratios. These copolymers were further cross-linked to form a biocompatible and biodegradable polymer-based vascular stent with excellent shape-memory effect functionality ($R_f \sim 100\%$, $R_r > 90\%$, and $R_t \leq 10$ s). The shape-memory behavior and degradation rate could be modulated by adjusting the weight ratio of PEG/PCL. The stent can also recover from a linear configuration to a spiral shape with a transition temperature around body temperature.

Mitomycin C was conjugated with and curcumin was coated to this stent to establish a shape-memory dual-drug-eluting stent (SMDES). The SMDES could sustainably release the anticoagulant drug (curcumin) over 14 days and the antiproliferation drug (mitomycin C) over 70 days. This combination of release profiles served to reduce platelet adhesion in the early stages and to suppress long-term hSMCs hyperproliferation while having a minimal effect on the viability of hUVECs. The cPEG-PCL_6040 stent maintained its integrity with a 47% weight loss after 2 months of flushing in a pulsatile bioreactor, suggesting that the cPEG-PCL_6040 stent did not collapse during the bulk degradation process. Our results demonstrate that cPEG-PCL_6040 SMDES has the potential for use as a thermo-induced, biodegradable stent implant for the treatment of coronary artery disease by preventing vascular restenosis following angioplasty.

ASSOCIATED CONTENT

Supporting Information

DSC curves of PCL-PEG_6040 block copolymer and cPCL-PEG_6040 stent. This material is available free of charge via the Internet at http://pubs.acs.org.

AUTHOR INFORMATION

Corresponding Author

*Tel: +886-3-5715131 ext 33856. Fax: +886-3-5722366. E-mail: twwang@mx.nthu.edu.tw.

Author Contributions

#These authors contributed equally.

Notes

The authors declare no competing financial interest.

REFERENCES

(1) Serruys, P. W.; Kutryk, M. J. B.; Ong, A. T. L. *N. Engl. J. Med.* **2006**, *354*, 483−495.
(2) van der Hoeven, B. L.; Pires, N. M. M.; Warda, H. M.; Oemrawsingh, P. V.; van Vlijmen, B. J. M.; Quax, P. H. A.; Schalij, M. J.; van der Wall, E. E.; Jukema, J. W. *Int. J. Cardiol.* **2005**, *99*, 9−17.
(3) Kibos, A.; Campeanu, A.; Tintoiu, I. *Acute Card. Care* **2007**, *9*, 111−119.
(4) Austin, G. E.; Ratliff, N. B.; Hollman, J.; Tabei, S.; Phillips, D. F. *J. Am. Coll. Cardiol.* **1985**, *6*, 369−735.
(5) Kraitzer, A.; Kloog, Y.; Zilberman, M. *J. Biomed. Mater. Res., Part B* **2008**, *85*, 583−603.
(6) Jang, H. S.; Nam, H. Y.; Kim, J. M.; Hahm, D. H.; Nam, S. H.; Kim, K. L.; Joo, J. R.; Suh, W.; Park, J. S.; Kim, D. K.; Gwon, H. C. *Catheter. Cardiovasc. Interventions* **2009**, *74*, 881−888.
(7) Nakazawa, G.; Finn, A. V.; Kolodgie, F. D.; Virmani, R. *Expert Rev. Med. Devices* **2009**, *6*, 33−42.
(8) Huang, Y.; Venkatraman, S. S.; Boey, F. Y. C.; Lahti, E. M.; Umashankar, P. R.; Mohanty, M.; Arumugam, S.; Khanolkar, L.; Vaishnav, S. *Biomaterials* **2010**, *31*, 4382−4391.
(9) Farb, A.; Heller, P. F.; Shroff, S.; Cheng, L.; Kolodgie, F. D.; Carter, A. J.; Scott, D. S.; Froehlich, J.; Virmani, R. *Circulation* **2001**, *104*, 473−479.
(10) Chen, M. C.; Chang, Y.; Liu, C. T.; Lai, W. Y.; Peng, S. F.; Hung, Y. W.; Tsai, H. W.; Sung, H. W. *Biomaterials* **2009**, *30*, 79−88.
(11) McFadden, E. P.; Stabile, E.; Regar, E.; Cheneau, E.; Ong, A. T. L.; Kinnaird, T.; Suddath, W. O.; Weissman, N. J.; Torguson, R.; Kent, K. M.; Pichard, A. D.; Satler, L. F.; Waksman, R.; Serruys, P. W. *Lancet* **2004**, *364*, 1519−1521.
(12) Lendlein, A.; Schmidt, A. M.; Langer, R. *Proc. Natl. Acad. Sci. U.S.A.* **2001**, *98*, 842−847.
(13) Lendlein, A.; Langer, R. *Science* **2002**, *296*, 1673−1676.
(14) Wilson, T. S.; Small, W. I. V.; Benett, W. J.; Bearinger, J. P.; Maitland, D. J. *Proc. SPIE* **2005**, *6007*, 157.
(15) Wischke, C.; Neffe, A. T.; Lendlein, A. *Shape-Mem. Polym. Adv. Polym. Sci.* **2010**, *226*, 177.
(16) Yakacki, C. M.; Shandas, R.; Lanning, C.; Rech, B.; Eckstein, A.; Gall, K. *Biomaterials* **2007**, *28*, 2255−2263.
(17) Kotsar, A.; Isotalo, T.; Mikkonen, J.; Juuti, H.; Martikainen, P. M.; Talja, M.; Kellomäki, M.; Törmälä, P.; Tammela, T. L. *J. Endourol.* **2008**, *22*, 1065−1069.
(18) Domingo, S.; Puértolas, S.; Gracia-Villa, L.; Puértolas, J. A. *Minimally Invasive Ther. Allied Technol.* **2007**, *16*, 126−136.
(19) Zhou, S.; Deng, X.; Yang, H. *Biomaterials* **2003**, *24*, 3563−3570.
(20) Treetharnmathurot, B.; Ovartlarnporn, C.; Wungsintaweekul, J.; Duncan, R.; Wiwattanapatapee, R. *Int. J. Phytorem.* **2008**, *357*, 252−259.
(21) Xiao, Y.; Zhou, S.; Wang, L.; Zheng, X.; Gong, T. *Composites, Part B* **2010**, *41*, 537−542.
(22) Iwasaki, K.; Kojima, K.; Kodama, S.; Paz, A. C.; Chambers, M.; Umezu, M.; Vacanti, C. A. *Circulation* **2008**, *118*, S52−S57.
(23) Xue, L.; Dai, S.; Li, Z. *Biomaterials* **2010**, *31*, 8132−8140.

(24) Venkatraman, S.; Poh, T. L.; Vinalia, T.; Mak, K. H.; Boey, F. *Biomaterials* **2003**, *24*, 2105−2111.
(25) Rechavia, E.; Litvack, F.; Fishbien, M. C.; Nakamura, M.; Eigler, N. *Catheter. Cardiovasc. Diagn.* **1998**, *45*, 202−207.
(26) Gan, Z.; Yu, D.; Zhong, Z.; Liang, Q.; Jing, X. *Polymer* **1999**, *40*, 2859−2862.
(27) Wei, X.; Gong, C.; Gou, M.; Fu, S.; Guo, Q.; Shi, S.; Luo, F.; Guo, G.; Qiu, L.; Qian, Z. *Int. J. Phytorem.* **2009**, *381*, 1−18.
(28) Nuutinen, J. P.; Clerc, C.; Reinikainen, R.; Törmälä, P. *J. Biomater. Sci., Polym. Ed.* **2003**, *14*, 255−266.
(29) Zilberman, M.; Schwade, N. D.; Eberhart, R. C. *J. Biomed. Mater. Res., Part B* **2004**, *69B*, 1−10.
(30) Weintraub, W. S. *Am. J. Cardiol.* **2007**, *100*, 3−9.
(31) Wagner, D. D.; Burger, P. C. *Arterioscler., Thromb., Vasc. Biol.* **2003**, *23*, 2131−2137.
(32) Axel, D. I.; Kunert, W.; Göggelmann, C.; Oberhoff, M.; Herdeg, C.; Küttner, A.; Wild, D. H.; Brehm, B. R.; Riessen, R.; Köveker, G.; Karsch, K. R. *Circulation* **1997**, *96*, 636−645.
(33) Pan, C. J.; Shao, Z. Y.; Tang, J. J.; Wang, J.; Huang, N. *J. Biomed. Mater. Res., Part A* **2007**, *82*, 740−746.
(34) Srivastava, R.; Dikshit, M.; Srimal, R. C.; Dhawan, B. N. *Thromb. Res.* **1985**, *40*, 413−417.
(35) Srivastava, R.; Puri, V.; Srimal, R. C.; Dhawan, B. N. *Arzneimittelforschung* **1986**, *36*, 715−717.
(36) Granada, J. F.; Ensenat, D.; Keswani, A. N.; Kaluza, G. L.; Raizner, A. E.; Liu, X. M.; Peyton, K. J.; Azam, M. A.; Wang, H.; Durante, W. *Arterioscler., Thromb., Vasc. Biol.* **2005**, *25*, 2343−2348.
(37) Wache, H. M.; Tartakowska, D. J.; Hentrich, A.; Wagner, M. H. *J. Mater. Sci.: Mater. Med.* **2003**, *14*, 109−112.
(38) Ju, F.; Xia, Z.; Sasaki, K. *J. Mech. Behav. Biomed. Mater.* **2008**, *1*, 86−95.
(39) Cardinal, K. O.; Bonnema, G. T.; Hofer, H.; Barton, J. K.; Williams, S. K. *Tissue Eng.* **2006**, *12*, 3431−3438.
(40) Ganesh, M.; Gross, R. A. *Polymer* **2012**, *53*, 3454−3461.
(41) Ramcharitar, S.; Serruys, P. W. *Am. J. Cardiovasc. Drugs* **2008**, *8*, 305−314.